Available online at www.sciencedirect.com
SCIENCE DIRECT
Journal of Molecular Catalysis A: Chemical 241 (2005) 227–232
JOURNAL OF MOLECULAR CATALYSIS A: CHEMICAL
www.elsevier.com/locate/molcata

UV–vis spectroscopy studies of $H_3PMo_{12-x}W_xO_{40}$ heteropolyacid (HPA) catalysts in the solid state: Effects of water content and polyatom substitution

Min Hye Youn [a], Heesoo Kim [a], Ji Chul Jung [a], In Kyu Song [a,*], Katherine P. Barteau [b], Mark A. Barteau [b]

[a] *School of Chemical and Biological Engineering, Seoul National University, Shinlim-dong, Kwanak-ku, Seoul 151-744, Republic of Korea*
[b] *Department of Chemical Engineering, University of Delaware, Newark, DE 19716, USA*

Received 16 June 2005; received in revised form 15 July 2005; accepted 16 July 2005
Available online 22 August 2005

Abstract

UV–vis spectra of solid state $H_3PMo_{12-x}W_xO_{40}$ ($x = 0, 3, 6, 9, 12$) catalysts were obtained to elucidate the effect of crystalline water molecules and to explore the reduction potentials of the heteropolyacid (HPA) catalysts. The UV–vis spectra of HPA catalysts in the solid state varied in a systematic way depending on the number of crystalline water molecules (depending on the treatment temperature). Absorption edges of solid HPA catalysts shifted to longer wavelength (to lower edge energy) with decreasing the number of crystalline water molecules (with increasing treatment temperature). Absorption edge energies of $H_3PMo_{12-x}W_xO_{40}$ catalysts treated under consistent conditions shifted to higher values with increasing the number of (more electronegative) tungsten atoms in the framework. The absorption edge energies of the $H_3PMo_{12-x}W_xO_{40}$ catalysts were directly correlated with their reduction potentials. A lower absorption edge energy corresponded to a higher reduction potential of the HPA. The absorption edge energies determined from UV–vis spectroscopy of HPAs in the solid state could be utilized as a correlating parameter for the reduction potentials of these catalysts.

Keywords: UV–vis spectroscopy; Heteropolyacid; Dehydration; Reduction potential; Absorption edge energy

1. Introduction

Heteropolyacids (HPAs) have attracted much attention as oxidation catalysts [1–5]. Fundamental understanding of the reduction potential (oxidizing power) of HPA catalysts is of great importance in designing HPA catalysts for selective oxidation reactions. To determine the reduction potential of HPA catalysts, various theoretical and instrumental techniques have been employed. These examples include quantum chemical molecular orbital studies [6,7], electrochemical measurements in solutions [8–11] and scanning tunneling microscopy (STM) investigations of HPA self-assembled monolayers for the determination of negative differential resistance (NDR) peak voltages [12–15]. Another promising approach to probe the reduction potentials of HPA catalysts is to measure the absorption edges from UV–vis spectra of HPAs [16]. It has been demonstrated that HPA catalysts with higher reduction potentials exhibited absorption edges at longer wavelengths in their UV–vis spectra in solution. It was also revealed that absorption edges determined from UV–vis spectra of solid HPA catalysts may serve as a correlating parameter for the reduction potentials of the HPA catalysts [17,18]. A previous work [19] has demonstrated the correlation of absorption edges with catalyst activity of vanadium oxide catalysts for isobutane oxidative dehydrogenation, where UV–vis spectroscopy was used to probe the extent of reduction of vanadium oxides during this reaction [19].

Absorption edges in the UV–vis spectrum of an HPA catalyst measure the energy required for electron transfer from the highest occupied molecular orbital (HOMO) to the lowest unoccupied molecular orbital (LUMO) [20]. The HOMO energy is not greatly affected by changes in the HPA framework, while the LUMO energy is greatly affected by framework polyatom substitution [7,21]. The band gap energy between the HOMO and the LUMO of an HPA catalyst reflects the reduction potential

* Corresponding author. Tel.: +82 2 880 9227; fax: +82 2 888 7295.
E-mail address: inksong@snu.ac.kr (I.K. Song).

1381-1169/$ – see front matter © 2005 Elsevier B.V. All rights reserved.
doi:10.1016/j.molcata.2005.07.023

of the HPA catalyst. The smaller band gap energy corresponds to the higher reduction potential of the HPA catalyst [7,21]. It is believed that the effect of framework polyatom substitution on the band gap energy variation, i.e. on the reduction potential, can be probed by UV–vis spectroscopy.

Reported in this work is UV–vis spectroscopy studies of solid $H_3PMo_{12-x}W_xO_{40}$ ($x = 0$, 3, 6, 9, 12) HPA catalysts to elucidate the effect of crystalline water molecules and to explore the reduction potentials of the HPA catalysts. This is a typical example showing how one can characterize the fundamental catalytic properties of solid state HPA catalysts by simple UV–vis spectroscopy measurements. In particular, this work demonstrates how one can probe the reduction potentials of solid state HPA catalysts by UV–vis spectroscopy measurements.

2. Experimental

2.1. Materials and thermal analyses

Commercially available $H_3PMo_{12-x}W_xO_{40}$ ($x = 0, 3, 6, 9, 12$) HPA catalysts were purchased from Sigma–Aldrich Chemical Co. and Nippon Inorganic Colors and Chem. Each solid HPA sample was kept in an open space under ambient conditions for 2 days to absorb reversibly as much water as it can. The TGA spectrum of each HPA was obtained with a TGA-50 instrument (Shimadzu) with a heating rate of 10 °C/min to determine the pre-treatment temperatures necessary for dehydration of each catalyst.

2.2. UV–vis spectroscopy measurements

In order to determine the effect of crystalline water molecules on the UV–vis spectra, the HPA catalysts were thermally treated at various temperatures on the basis of the TGA results. UV–vis spectra of solid state $H_3PMo_{12-x}W_xO_{40}$ ($x = 0$, 3, 6, 9, 12) HPA catalysts were obtained with a Lambda-35 spectrometer (Perkin-Elmer). The Kubelka–Munk function ($F(R_\infty)$) was used to convert reflectance measurements into equivalent absorption spectra using the reflectance of $BaSO_4$ as a reference [22], and to obtain absorption edge energies directly from the $[F(R_\infty)h\nu]^{1/2}$ curves.

3. Results and discussion

3.1. TGA and UV–vis spectra of solid $H_3PW_{12}O_{40}$

Fig. 1 shows the TGA spectrum of $H_3PW_{12}O_{40}$. The HPA catalyst lost weight continuously with increasing temperature due to the removal of crystalline water molecules, and finally started to decompose at around 550 °C (according to the DTA spectrum, not shown here), in good agreement with a previous report [23]. Weight loss in the low temperature region (<180 °C) was much smaller than that at higher temperatures. Although the exact number of water molecules removed from $H_3PW_{12}O_{40}$ was not quantitatively determined, it is clear that $H_3PW_{12}O_{40}$ catalyst experienced relatively little dehydration in the low temperature region.

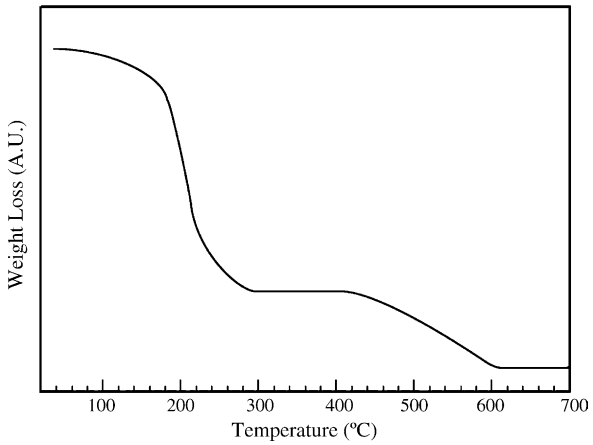

Fig. 1. TGA spectrum of $H_3PW_{12}O_{40}$.

Fig. 2 shows the UV–vis spectra of $H_3PW_{12}O_{40}$ treated at various temperatures. The treatment temperatures were chosen on the basis of the TGA results. It should be noted that UV–vis spectra of solid $H_3PW_{12}O_{40}$ varied in a systematic way depending on the treatment temperature. That is, UV–vis spectra of the HPA catalyst were affected in a consistent fashion by the number of crystalline water molecules. What is important is that the UV–vis spectra of $H_3PW_{12}O_{40}$ catalyst shifted to longer wavelength with increasing treatment temperatures (with decreasing crystalline water molecules). This is consistent with the observation that the absorption edge wavelengths of solid HPA catalysts were consistently longer than those of the corresponding HPA solution samples [16].

3.2. Effect of dehydration on edge energy of solid $H_3PW_{12}O_{40}$

In order to find a correlation between absorption edge energy and treatment temperature of $H_3PW_{12}O_{40}$, absorption edge energies were directly determined from the profiles derived from the Kubelka–Munk function [22]. Fig. 3 shows the $[F(R_\infty)h\nu]^{1/2}$ curves of solid $H_3PW_{12}O_{40}$ treated at various temperatures. Absorption edge energies were determined by the intercept

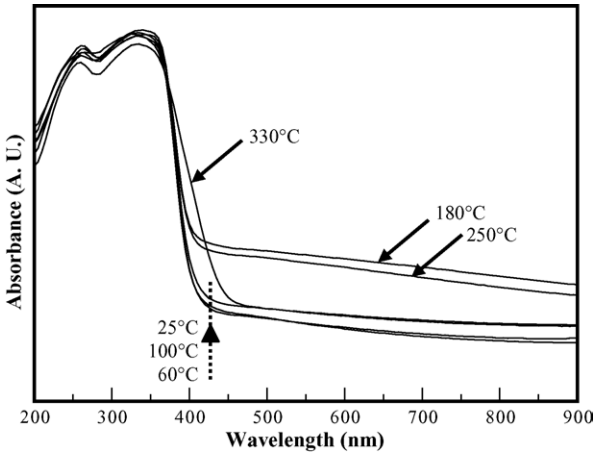

Fig. 2. UV–vis spectra of $H_3PW_{12}O_{40}$ treated at various temperatures.

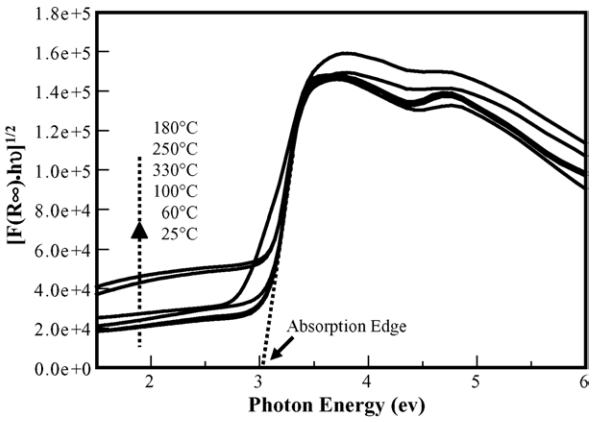

Fig. 3. $[F(R_\infty)h\nu]^{1/2}$ curves of $H_3PW_{12}O_{40}$ treated at various temperatures.

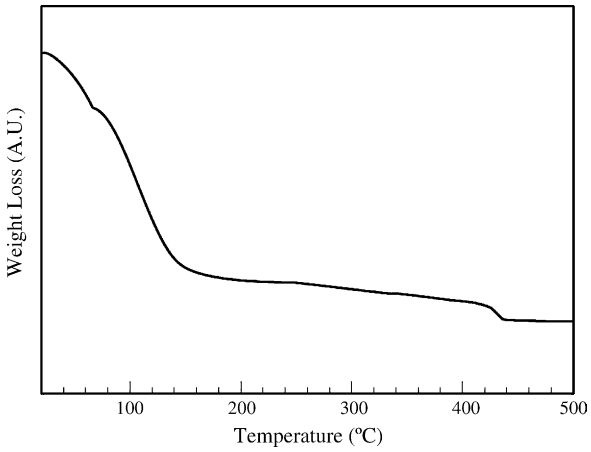

Fig. 5. TGA spectrum of $H_3PMo_{12}O_{40}$.

of a linear fit to the absorption edge. Fig. 4 shows the correlation between edge energy and dehydration temperature of $H_3PW_{12}O_{40}$. The correlation profile in Fig. 4 was very similar to the TGA profile in Fig. 1. The variation of edge energy at low temperatures was much smaller than that at the high temperature region, consistent with the TGA result, which showed that fewer water molecules were lost below 180 °C. At the high temperature region, where the larger amounts of water molecules desorbed, the $H_3PW_{12}O_{40}$ sample exhibited a significant decrease in edge energies. This result demonstrates that UV–vis spectrum of the solid HPA catalyst was strongly affected by the number of crystalline water molecules, that is, by the thermal treatment, in a similar fashion observed for typical semi-conducting materials [17,24].

3.3. Effect of water molecules in solid $H_3PMo_{12}O_{40}$

The effect of water molecules on the UV–vis spectra of solid HPA catalysts was also confirmed by examining $H_3PMo_{12}O_{40}$. Fig. 5 shows the TGA spectrum of $H_3PMo_{12}O_{40}$. The HPA catalyst lost weight continuously with increasing temperature due to the removal of crystalline water molecules, and was finally decomposed at around 430 °C (DTA spectrum not shown here), in good agreement with a previous report [23]. Unlike the $H_3PW_{12}O_{40}$ sample, weight loss of $H_3PMo_{12}O_{40}$ in the low temperature region (<150 °C) was much larger than that in the high temperature region. The $H_3PMo_{12}O_{40}$ catalyst experienced considerable dehydration in the low temperature region.

Fig. 6 shows the correlation between edge energy determined from the $[F(R_\infty)h\nu]^{1/2}$ curve and the treatment temperature of solid $H_3PMo_{12}O_{40}$. One again, the edge energy profile versus temperature in Fig. 6 resembled the TGA profile in Fig. 5. The variation of edge energy in the low temperature region was much larger than that in the high temperature region, consistent with the TGA result, which showed extensive dehydration at below 150 °C. This result also demonstrates that UV–vis spectrum of solid $H_3PMo_{12}O_{40}$, like that of $H_3PW_{12}O_{40}$ was strongly affected by the number of crystalline water molecules. However, since dehydration occurs at different temperatures for different HPAs, some caution is required in comparing results obtained for different materials at arbitrary temperatures.

The role and effect of water molecules on the catalytic properties of solid state HPA catalysts were also well characterized by NMR [25], ESR [26] and theoretical calculation [27]. In the ^1H MAS NMR spectroscopy study for $H_3PW_{12}O_{40}\cdot nH_2O$ at room temperature, three different states of protons were detected [25].

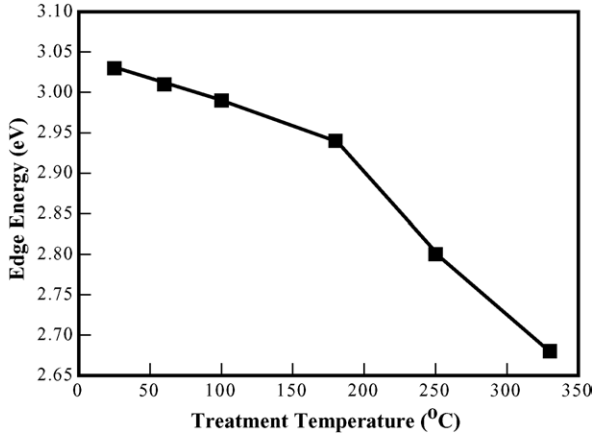

Fig. 4. Correlation between absorption edge energy and treatment temperature of $H_3PW_{12}O_{40}$.

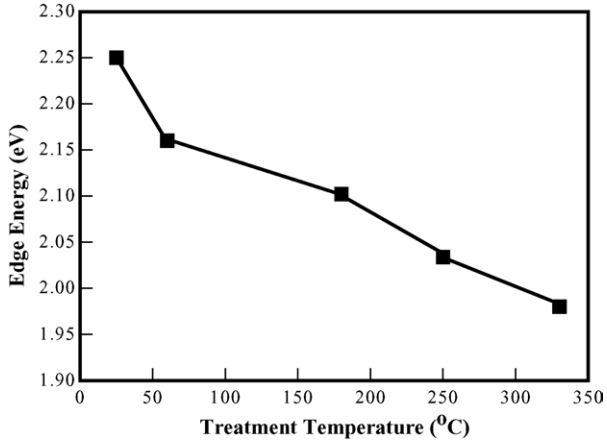

Fig. 6. Correlation between absorption edge energy and treatment temperature of $H_3PMo_{12}O_{40}$.

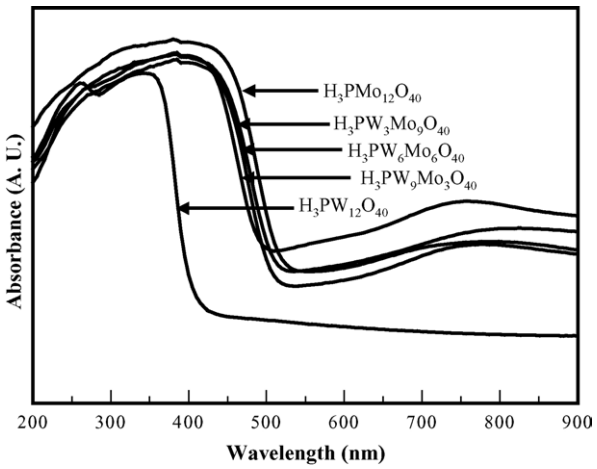

Fig. 7. UV–vis spectra of $H_3PMo_{12-x}W_xO_{40}$ ($x = 0, 3, 6, 9, 12$) catalysts treated at room temperature (25 °C).

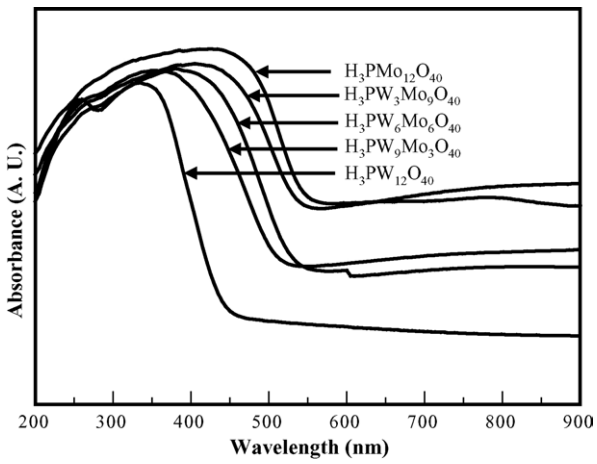

Fig. 9. UV–vis spectra of $H_3PMo_{12-x}W_xO_{40}$ ($x = 0, 3, 6, 9, 12$) catalysts treated at 330 °C.

In the ESR study for solid state $H_3PMo_{12}O_{40}$ catalyst reduced by H_2, it was reported that heat treatment eliminated oxide ions from heteropolyanion and led to development of Mo^{5+} signal, indicating the localization of electrons [26]. The interaction of anhydrous $H_3PW_{12}O_{40}$ with water molecules was also well elucidated by density functional theory (DFT) quantum chemical calculation [27].

3.4. UV–vis spectra and edge energies of $H_3PMo_{12-x}W_xO_{40}$ ($x = 0, 3, 6, 9, 12$)

Fig. 7 shows the UV–vis spectra of $H_3PMo_{12-x}W_xO_{40}$ ($x = 0$, 3, 6, 9, 12) catalysts treated at room temperature (25 °C). These HPAs exhibited characteristic differences in their UV–vis spectra. Absorption edges of $H_3PMo_{12-x}W_xO_{40}$ catalysts shifted to longer wavelengths with decreasing tungsten substitution (with increasing molybdenum substitution). Fig. 8 shows the $[F(R_\infty)h\nu]^{1/2}$ curves of $H_3PMo_{12-x}W_xO_{40}$ catalysts treated at room temperature (25 °C). A systematic variation of edge energies was also observed. Absorption edge energies of $H_3PMo_{12-x}W_xO_{40}$ catalysts increased with increasing tungsten substitution (with decreasing molybdenum substitution).

To elucidate the effect of water molecules, and in turn, to minimize the effect of water molecules, $H_3PMo_{12-x}W_xO_{40}$ catalysts were thermally treatment at 330 °C before UV–vis spectra of these samples were taken. TGA and DSC measurements confirmed that this temperature was sufficient to remove the bulk of the crystalline water in each case without causing decomposition of any sample. Fig. 9 shows the UV–vis spectra of $H_3PMo_{12-x}W_xO_{40}$ catalysts treated at 330 °C. Absorption edges of $H_3PMo_{12-x}W_xO_{40}$ catalysts treated at 330 °C shifted to longer wavelengths with decreasing tungsten substitution (with increasing molybdenum substitution), in the same fashion as (but with greater separation between absorption spectra of different compounds than) those of $H_3PMo_{12-x}W_xO_{40}$ catalysts treated at 25 °C. It is noticeable that absorption edges of HPA catalysts treated at 330 °C appeared at longer wavelengths in all cases than those of HPAs treated at 25 °C, in good agreement with the result in Fig. 2. Fig. 10 shows the $[F(R_\infty)h\nu]^{1/2}$ curves of $H_3PMo_{12-x}W_xO_{40}$ (0, 3, 6, 9, 12) catalysts treated at 330 °C. The HPA catalysts showed a systematic variation in absorption edge energies. Absorption edge energies of the HPA catalysts treated at 330 °C also increased with increasing tungsten substitution (with decreasing molybdenum substitution). This trend

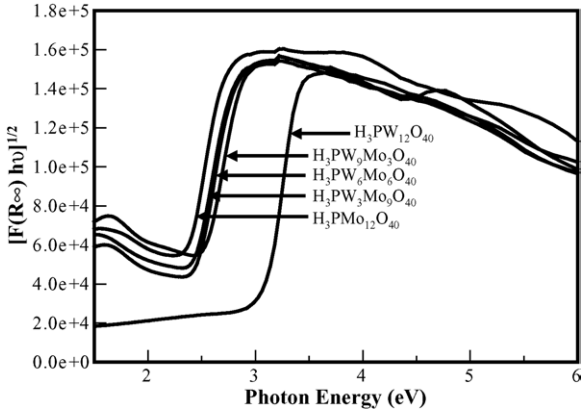

Fig. 8. $[F(R_\infty)h\nu]^{1/2}$ curves of $H_3PMo_{12-x}W_xO_{40}$ ($x = 0, 3, 6, 9, 12$) catalysts treated at room temperature (25 °C).

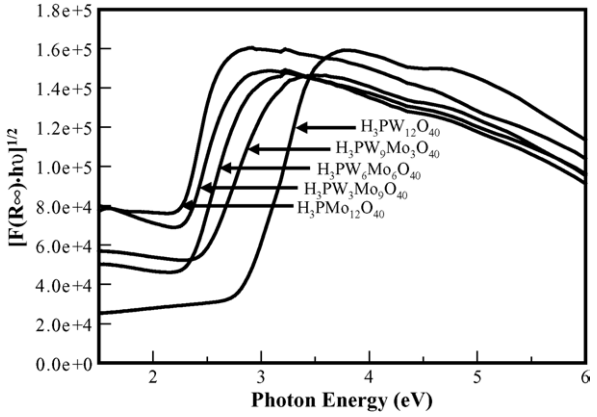

Fig. 10. $[F(R_\infty)h\nu]^{1/2}$ curves of $H_3PMo_{12-x}W_xO_{40}$ ($x = 0, 3, 6, 9, 12$) catalysts treated at 330 °C.

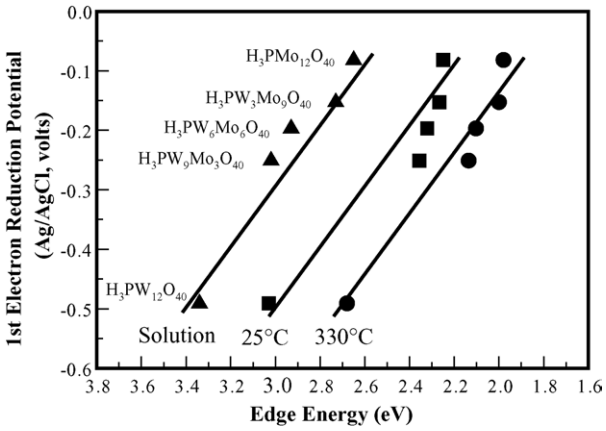

Fig. 11. Correlation between absorption edge energy and reduction potential of $H_3PMo_{12-x}W_xO_{40}$ ($x = 0, 3, 6, 9, 12$) catalysts. Solid HPAs were treated at 25 °C (squares) and 330 °C (circles) for the UV–vis spectroscopy measurements. Edge energies determined by direct extrapolation of the absorption spectra of aqueous (0.01 M) solutions of these HPAs (triangles) were taken from reference [16].

was well consistent with that observed for $H_3PMo_{12-x}W_xO_{40}$ catalysts treated at 25 °C (Fig. 8), as well as that observed for aqueous solutions of these compounds [16].

3.5. Edge energy as a correlating parameter for reduction potentials of $H_3PMo_{12-x}W_xO_{40}$

Fig. 11 shows the correlation between absorption edge energies and reduction potentials of $H_3PMo_{12-x}W_xO_{40}$ ($x = 0, 3, 6, 9, 12$) catalysts. Absorption edge energies of $H_3PMo_{12-x}W_xO_{40}$ catalysts measured after thermal treatment at 25 °C (Fig. 8) and 330 °C (Fig. 10) were represented in Fig. 11. Reduction potential data for the $H_3PMo_{12-x}W_xO_{40}$ catalysts from electrochemical measurements in solution were taken from a previous report [11]. The trends of reduction potentials of $H_3PMo_{12-x}W_xO_{40}$ catalysts in the reference [11] were quite consistent with those determined from quantum-chemical molecular orbital [7] and scanning tunneling microscopy studies [15,28]. Molecular orbital studies [7,21] for polyatom-substituted HPA catalysts revealed that the energy gap between the HOMO and the LUMO was consistent with the reduction potential of the HPAs; the more reducible HPAs showed smaller energy gaps. Those studies [7,21] also showed that electrons added to the polyatom-substituted HPAs were localized on the less electronegative metal center (note that molybdenum is less electronegative than tungsten). It is inferred that the less electronegative polyatom in the $H_3PMo_{12-x}W_xO_{40}$ catalysts was much more efficient in the role of electron localization. Therefore, the reduction potential of $H_3PMo_{12-x}W_xO_{40}$ ($x = 0, 3, 6, 9, 12$) catalysts increased with decreasing the number of more electronegative tungstens in the framework.

As shown in Fig. 11, the absorption edge energies of the HPA catalysts could be directly correlated with the reduction potentials of the polyatom-substituted HPA catalysts. Reduction potentials of $H_3PMo_{12-x}W_xO_{40}$ catalysts increased with decreasing edge energies of the HPA catalysts in both cases. The edge energy lines measured after thermal treatment at 25 and 330 °C were parallel to each other. This implies that the absorption edge energies of HPAs measured at consistent extents of dehydration may serve as a correlating parameter for the reduction potentials of these solid catalysts. Similar correlations appear to hold for the reduction potentials of HPA catalysts with the absorption edges measured in aqueous solution [16].

In an aqueous solution, heteropolyacids are dissociated and the heteropolyanions fully solvated by water molecules. Therefore, UV–vis spectra of HPAs at constant concentration in solution may give directly comparable results. On the other hand, UV–vis spectra of solid HPAs appeared to be sensitive to the number of coordinated water molecules, as revealed in this work. This may be understood by the fact that solid HPA catalysts form flexible secondary structures depending on the identity of substituted metal species and the number of crystalline water molecules. Therefore, some caution is required in characterizing the solid HPA catalysts by UV–vis spectroscopy. Comparison of catalytic properties of solid HPA catalysts probed by UV–vis spectroscopy should be made under consistent conditions of hydration, these are most easily achieved by utilizing well hydrated or well dehydrated samples, rather than by relying on treatment at consistent temperatures if these are intermediate along the dehydration profile.

4. Conclusions

UV–vis spectroscopy studies of solid $H_3PMo_{12-x}W_xO_{40}$ ($x = 0, 3, 6, 9, 12$) catalysts were carried out to determine the effect of crystalline water molecules and to explore correlations with the reduction potentials of these catalysts. The UV–vis spectra of solid HPAs varied in a systematic way depending on the number of crystalline water molecules. Absorption edges of solid HPAs shifted to longer wavelength (to lower edge energy) with decreasing numbers of crystalline water molecules (with increasing treatment temperature). The dehydration profiles of solid HPA catalysts were very similar to the absorption edge profiles plotted with respect to treatment temperatures. Absorption edge energies of $H_3PMo_{12-x}W_xO_{40}$ catalysts treated under consistent conditions shifted to higher values with increasing the number of more electronegative tungsten atoms substituted in the framework. The absorption edge energies of the $H_3PMo_{12-x}W_xO_{40}$ catalysts could be directly correlated with the reduction potentials of the HPA catalysts. HPA catalysts with higher reduction potentials showed lower edge energies in UV–vis spectra. Thus, the absorption edge energy determined from the UV–vis spectrum of a solid HPA catalyst under consistent conditions may serve as a correlation parameter for its reduction potential.

Acknowledgement

The authors acknowledge the support from KOSEF (R01-2004-000-10502-0).

References

[1] M. Misono, Catal. Rev. Sci. Eng. 29 (1987) 269.

[2] H.C. Kim, S.H. Moon, W.Y. Lee, Chem. Lett. (1991) 447.
[3] I.V. Kozhevnikov, Catal. Rev. Sci. Eng. 37 (1995) 311.
[4] C.L. Hill, C.M. Prosser-McCartha, Coord. Chem. Rev. 143 (1995) 407.
[5] M.A. Barteau, J.E. Lyons, I.K. Song, J. Catal. 216 (2003) 236.
[6] K. Eguchi, T. Seiyama, N. Yamazoe, S. Katsuki, H. Taketa, J. Catal. 111 (1988) 336.
[7] R.S. Weber, J. Phys. Chem. 98 (1994) 2999.
[8] M.T. Pope, G.M. Varga Jr., Inorg. Chem. 5 (1966) 1249.
[9] J.J. Altenau, M.T. Pope, R.A. Prados, H. So, Inorg. Chem. 14 (1975) 417.
[10] B. Keita, L. Nadjo, Mater. Chem. Phys. 22 (1989) 77.
[11] I.K. Song, M.A. Barteau, J. Mol. Catal. A 212 (2004) 229.
[12] M.S. Kaba, I.K. Song, M.A. Barteau, J. Phys. Chem. 100 (1996) 19577.
[13] M.S. Kaba, I.K. Song, M.A. Barteau, J. Vac. Sci. Technol. A 15 (1997) 1299.
[14] I.K. Song, M.A. Barteau, J. Mol. Catal. A 182–183 (2002) 185.
[15] I.K. Song, M.A. Barteau, Langmuir 20 (2004) 1850.
[16] K.P. Barteau, J.E. Lyons, I.K. Song, M.A. Barteau, Top. Catal., submitted for publication.
[17] J. Melsheimer, S.S. Mahmoud, G. Mestl, R. Schlögl, Catal. Lett. 60 (1999) 103.
[18] M.H. Youn, H. Kim, I.K. Song, K.P. Barteau, M.A. Barteau, React. Kinet. Catal. Lett., in press.
[19] M.D. Argyle, K. Chen, C. Resini, C. Krebs, A.T. Bell, E. Iglesia, J. Phys. Chem. B 108 (2004) 2345.
[20] T. Yamase, Chem. Rev. 98 (1998) 307.
[21] J.M. Maestre, X. Lopez, C. Bo, J.-M. Poblet, N. Casan-Pastor, J. Am. Chem. Soc. 123 (2001) 3749.
[22] P. Kubelka, F. Munk, Z. Tech. Phys. 12 (1931) 593.
[23] T. Okuhara, N. Mizuno, M. Misono, Adv. Catal. 41 (1996) 113.
[24] R.S. Weber, J. Catal. 151 (1995) 470.
[25] Y. Kanda, K.Y. Lee, S. Nakata, S. Asaoka, M. Misono, Chem. Lett. (1988) 139.
[26] N. Mizuno, K. Katamura, Y. Yoneda, M. Misono, J. Catal. 83 (1983) 384.
[27] M.J. Janik, K.A. Campbell, B.B. Bardin, R.J. Davis, M. Neurock, Appl. Catal. A 256 (2003) 51.
[28] I.K. Song, M.S. Kaba, M.A. Barteau, W.Y. Lee, Catal. Today 44 (1998) 285.